NANOSTRUCTURED BACK SIDE SILICON SOLAR CELLS

P. Voisin[1], M. Peters[1], H. Hauser[1], C. Helgert[2], E.-B. Kley [2], T. Pertsch[2], B. Bläsi[1], M. Hermle[1], S. W. Glunz[1]
[1] Fraunhofer Institute for Solar Energy Systems (ISE), Heidenhofstrasse 2, 79110 Freiburg, Germany
[2] Institute of Applied Physics, Friedrich-Schiller-Universität, Max-Wien-Platz 1, 07743 Jena, Germany
Tel +49 761/4588-5201, Fax +49 761/4588-9000, Email: Pauline.Voisin@ise.fraunhofer.de

ABSTRACT: In this paper, we report our investigation on the light trapping enhancement of silicon solar cells via the introduction of nanoscale gratings on the back side of solar cells. The grating is designed to diffract long wavelengths, typically from 900 nm to 1100 nm, leading to an enhancement of the photons path length in the solar cell. Therefore, a gain in current and then efficiency can be expected. The optimal grating parameters were first calculated via RCWA simulations, and were found to be a period of 310 nm for a flat front side and 410 nm for a textured front side. Test structures, with flat and textured front and back side and various silicon dioxide thicknesses on the back side, were then fabricated to confirm the simulation results. Reflection measurements performed on these test structures show a decrease of the reflection in that particular wavelength range for a flat front side. However, spectral response measurements of solar cells will be the only characterisation that can assure us that this decrease in reflection is inducing an increase of absorption in the silicon, as expected by simulation and not in the aluminium layer.

Keywords: silicon solar cells, light trapping, nanostructure, grating

1 INTRODUCTION

Light trapping enhancement is a key issue in silicon solar cells in order to reach high efficiencies. This includes the optimisation of the front side texturing [1] and anti reflection coatings [2], which both reduce the reflection (mainly on short wavelength). However, in order to absorb a maximal number of photons in the silicon wafer, which thickness is limited to a couple of hundred of microns, a lot of effort is made in order to increase the reflection on long wavelength by introducing perfect reflectors on the back side of solar cell [3, 4].

By focusing the increase of the optical path on these long wavelengths, more carriers can be generated within the solar cell, leading to an increase of the current and therefore also the efficiency. The employment of submicron gratings on the back side of silicon solar cells is an interesting and promising approach to reach this goal [5, 6]. Therefore, we focus our study on the effective path length enhancement via diffraction of long wavelengths by the introduction of a nanostructured Si/SiO_2 grating on the back side of monocrystalline silicon solar cells. This diffraction should lead to a reduction of the measured reflection on long wavelength. But contrary to standard reflectors, where the decrease in reflection is associated to a decrease in absorption in silicon, here the decrease in reflection should lead to an increase of absorption in silicon.

2 DEFINITION OF THE GRATING PARAMETERS

2.1 Simulations

To simulate the grating parameters, a semi analytical model based on the Rigorous Coupled Wave Analysis (RCWA) method was used. With the RCWA, the efficiencies and directions of the diffracted light in the solar cell were calculated. With these values, the absorption in the silicon was obtained and weighted with the AM1.5g spectrum. This procedure results in a measure for the current density produced by the solar cell, which exhibits a Si/SiO_2 grating covered by an aluminium reflector on the back side. This current was compared to the current density produced by a solar cell without grating (the back side reflector is composed of a dielectric-aluminium mirror stack). The parameter towards which the grating parameters were optimized was the difference between the current densities, the so called “gain in current density”. As only the first rear reflection is accounted, the method underestimates the total path and therefore also the gain in current density. The method therefore does not allow a correct estimation of the gain to be expected from the grating, meaning that the absolute value is also underestimated. The aim of the approach to include a grating was to increase the pathlength of the weakly absorbed light in the long wavelength regime. For that reason the optimization was performed only for the spectral range between 900 nm and 1127 nm. The graph presented Figure 1 shows the estimated gain in current density calculated on the 900-1127 nm wavelength range by simulation.

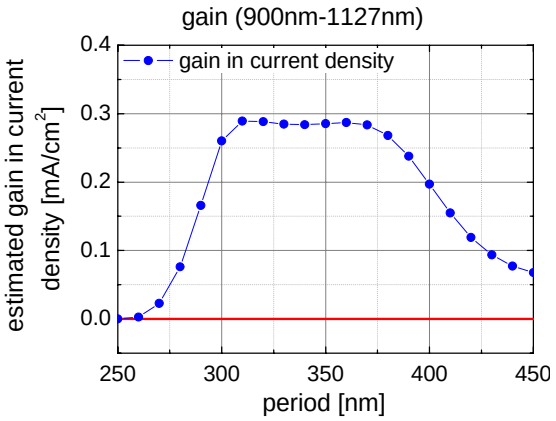

Figure 1: Optimization of the grating period for a flat front side solar cell with a grating on the back side. For this kind of grating a plateau exists for periods between 300 nm and 380 nm.

2.2 Gratings parameters

Using the method described in the last section, we calculated initial grating parameters that were used in a first experimental realisation. We calculated the parameters for two grating setups, one in which the front surface was flat and one for which the front surface was pyramidally textured. For the pyramidal texture, it needs to be considered, that the light impinges on the grating with different azimuthal orientations. Remarkable is, that the orientation in which the light is tilted by 90° towards the orientation in which the grating is periodical contributes most to the current gain. Correspondingly, the optimization of the grating period was performed towards this orientation. The optimum parameters calculated with the method for the two solar cell setups are given in Table I, the space to line ratio for both setups being 1:1.

	Optimum Depth	Optimum period
Flat front side	130 nm	310 nm
Textured front side	130 nm	410 nm

Table I: Optimised grating parameters for two solar cell setups. Optimised were grating depth and period.

3 EXPERIMENTS

3.1 Test structures

In order to confirm experimentally the simulation results, four test structures have been fabricated. Schematics of these test structures are presented in Figure 2. They combine flat or textured front side with inverted pyramids and flat or nanostrucuted back side. Due to experimental limitations for this batch, the gratings were fabricated with only one period and the optimum period for flat front side was chosen. Moreover, it is important to notice that every fabrication step has an effect on the morphological and electrical characteristics of the solar cell. For example, a thermal oxidation, which is used to passivate the surfaces, modifies the shape of the gratings. On the contrary, a deposited oxide does not modify the shape of the grating but also does not passivate the surface as good as a thermal oxide. Therefore, we used the same processes to fabricate these test structures as the ones used to fabricate solar cells in order to be as close as possible to the final solar cells.

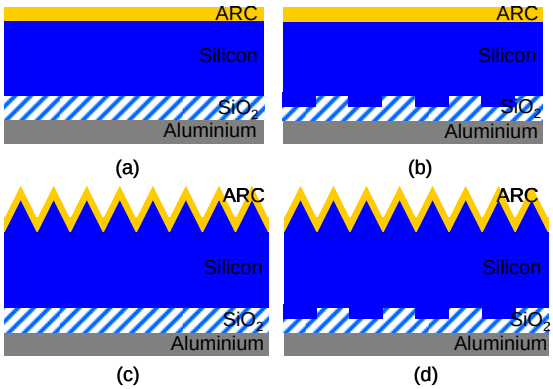

Figure 2: Schematic of the test structures (a) flat front and back side, (b) flat front side and nanostructured back side, (c) textured front side and flat back side and (d) textured front side and nanostructured back side.

3.2 Experimental details

The starting material is *p*-type, FZ, 1 Ωcm, 250 µm thick, monocrystalline [100] 4 inches silicon wafer. The nanogratings are first fabricated via electron-beam lithography (EBL), followed by an inductively coupled plasma etching step of the silicon. Although EBL is an expensive and costly technique, it is a flexible technology, which can easily fabricate sub micrometer patterns and thus allow us to demonstrate the feasibility of the global cell fabrication. This technique can be easily replaced in the future by a more cost- and industry-friendly structuring technique such as Nanoimprint Lithography [7].

A Scanning Electron Micrograph (SEM) of the grating at this stage is presented in Figure 3 (a). The grating has a period of 320 nm (190 nm lines and 130 nm space), and is 190 nm deep. The depth and space to line ratio are not yet in agreement with the values calculated by simulation, but we expect a modification of the morphology of the gratings with the following steps.

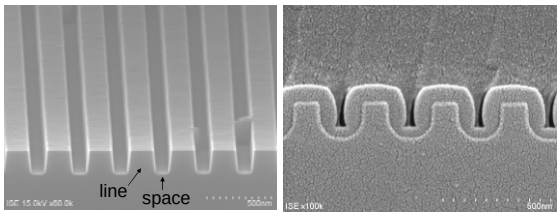

(a) (b)

Figure 3: Scanning Electron Micrographs (SEM) of the nanograting (a) etched in silicon and (b) after the thermal oxidation step.

A 105 nm thick thermal oxide is subsequently grown on both sides. This oxide is used on the one hand as a masking oxide for the fabrication of the inverted pyramids on the front side, and on the other hand as a passivation layer on the back side of the test samples. As it can be seen on the SEM picture (b) from Figure 3, this oxidation step strongly modifies the morphology of the grating. The period of the grating remains identical, but the line shrinks to 115 nm and the space increases to 205 nm. The height of the grating also reduces to 165 nm. It can be noticed that the optimal depth and space to line ratio are still not reached after oxidation, as the line width shrank more than expected and the depth less than expected. Further development is needed for this fabrication step. After a photolithographic step to align the front side texture to the back side one, and a wet chemical etching in KOH to fabricate the inverted pyramids, the front side is passivated with a 10 nm thermal oxide, and a 60 nm thick Silicon Nitride (SiN) Anti-Reflection Coating (ARC) is deposited by Plasma Enhanced Chemical Vapour Deposition (PECVD).

Finally, silicon dioxide is deposited by PECVD on the back side of the test structures with various thicknesses. This leads to a total silicon dioxide thickness of 130 nm, 230 nm and 450 nm. This SiO_2 is then coated by a 2 µm thick layer of aluminium by evaporation. SEM pictures of these samples are shown in Figure 4.

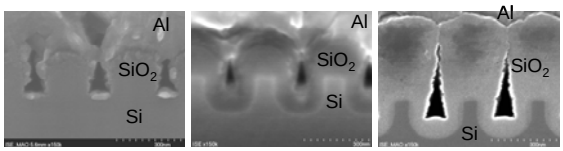

(a) (b) (c)

Figure 4: SEM pictures of the nanogratings with (a) 130 nm, (b) 230 nm and (c) 450 nm thick silicon dioxide between the silicon and aluminium reflector.

4 RESULTS AND DISCUSSION

The four test structures presented Figure 2, with the various thicknesses of SiO_2 were then optically characterized with a Fourier Spectrometer, on the 900 nm-1200 nm wavelength range, with unpolarised light. The graph presented Figure 5 compares the measured external reflection of flat front side samples, with flat and nanostructured backside. For the flat back side samples, only the measurement with 450 nm SiO_2 is shown, as for thicknesses above 130nm, the reflection does not depend on the SiO_2 thickness. For the nanostructured back side, the SiO_2 thickness variation is highlighted.

The same measurements performed on the samples with textured front side are presented in Figure 6. We observe for both types of setups, with flat or textured front side, a decrease in reflectance in the long wavelength region, and this for the various thicknesses of SiO_2 employed.

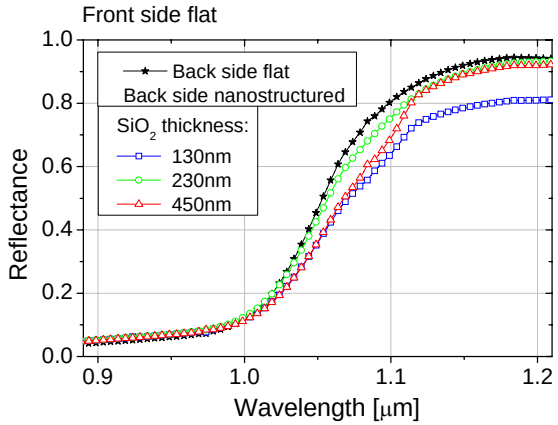

Figure 5: Front side reflection measured on 300 nm-1200 nm wavelength range on the test structures (a) and (b) from Figure 2, for various SiO_2 thicknesses.

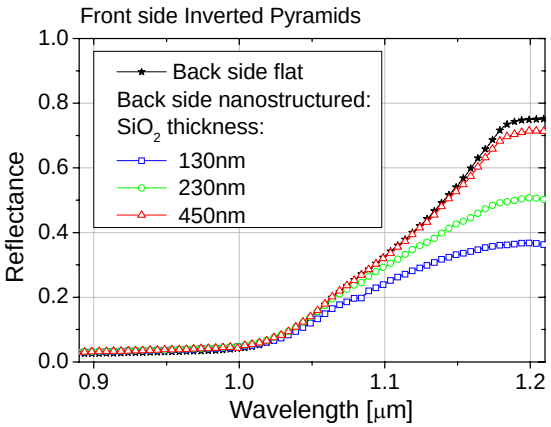

Figure 6: Front side reflection measured on 300 nm-1200 nm wavelength range on the test structures (c) and (d) from Figure 2, for various SiO_2 thicknesses.

From these measurements, the "reflectance reduction", calculated as the difference between the reflectance for a flat back side and the reflectance for a nanotextured back side, was calculated for the various front side and SiO_2 thicknesses. As it can be seen on the graph Figure 7, the samples with a flat front side (closed symbols) exhibit a peak of decrease in reflectance in the 1000 nm - 1120 nm wavelength range; and the samples with 130 nm of SiO_2 (squared symbols) exhibit a decrease in reflectance above 1120 nm.

However, the period of the gratings is optimised neither for a textured front side, nor for wavelengths longer than 1127 nm. Therefore, we expect no absorption enhancement in silicon and for this reason no reduction in reflection for these samples in these wavelength ranges. The decrease of reflection there, which is obviously happening, is then probably due parasitic absorption in the aluminium. When we observe closely the SEM picture of the samples with 130 nm thick SiO_2 (Figure 4a), it can be seen that some aluminium is also deposited in between the lines of the grating (the bright spots on the bottom of the spaces). Moreover, it is known that when a metallic layer is structured, there is an increase of absorption in it. Therefore, in that case, a decrease in reflectance would not lead to an increase of absorption in silicon. This situation should then be avoided.

For the samples with 450 nm thick SiO_2 (triangle symbols from Figure 7), hardly any reflectance reduction for textured samples can be seen, nor for the flat samples at wavelength higher than 1120 nm. This strengthen the assumption that all the decrease of reflection in 1000 nm – 1120 nm wavelength range could induce an increase of absorption in silicon. Furthermore, these measurements show that a thicker SiO_2 layer induces a flatter aluminium layer (see Figure 4c) and prevents the parasitic reflection reduction observed with a thinner dielectric layer. This optimal thickness will also in the future need to be determined.

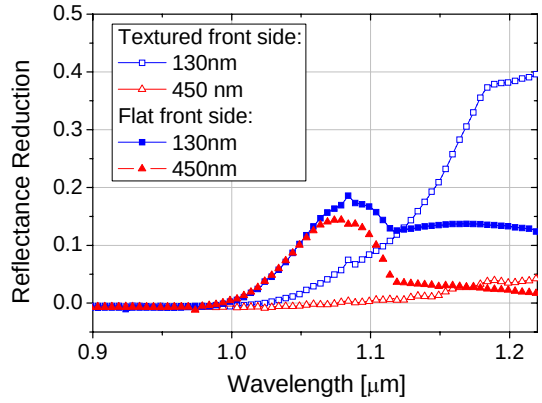

Figure 7: Reflectance reduction in the 900 nm-1200 nm wavelength range, calculated as the difference in reflection between the flat backside and the nanotextured one, for various front side and various SiO_2 thicknesses on the back side.

Finally, in order to compare this measured reflectance reduction to the absorption enhancement induced by the gratings calculated via simulation, both parameters are normalised to the flat reflection. The graph presented Figure 8 shows the relative reflection reduction measured on flat front side samples with 130 nm and 450 nm thick SiO_2 and the relative absorption enhancement calculated via simulation. This graph shows a good agreement between the simulation and the measurements in term of wavelength. Indeed, the decrease of reflection occurs at the same wavelength as the simulated gratings induce an increase of absorption. The mismatch in value between the measurement and the simulation probably results from the underestimation described paragraph 2.1.: the simulation calculates only two path of the light through the solar cell, although in reality many more occur. Finally, the highest decrease in reflection does not occur exactly at the same wavelength (1060-1070 nm) as the highest absorption enhancement does (1090 nm). This could be explained the difference in shape and period of the grating between the simulated gratings and the real ones.

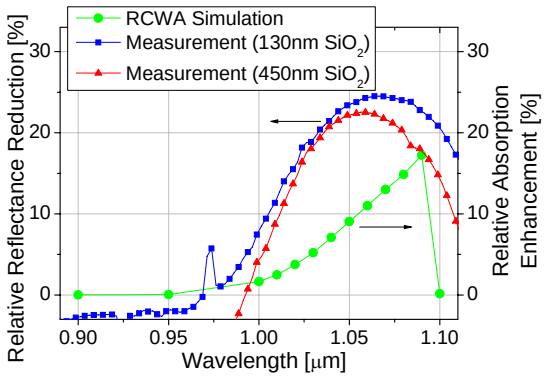

Figure 8: This graph shows a comparison between simulated relative absorption enhancement and measured relative reflection reduction for a solar cell with a backside grating.

Although we observe a decrease in reflection exactly on the wavelength range where the gratings are designed for, only spectral response measurement of solar cells build like these test structures can confirm us whether this reflection reduction induces an increase of absorption in the solar cell. Such solar cells and life time samples, which will evaluate the effect of the fabrication processes of the gratings on the electrical properties of the material, are currently under fabrication.

5 CONCLUSION

To conclude, we investigated the light trapping enhancement of silicon solar cells via the introduction of nanoscale gratings on their back side. With, RCWA simulations, it was found that the optimal grating parameters are a period of 310 nm for flat front side and 410 nm for textured one. Reflection measurements performed on test structures with flat front side show a decrease in reflection in the 1000 nm-1120 nm wavelength range, which is the range where the gratings are designed for. Therefore, this could be linked to an increase of absorption in silicon. However, in order to confirm this hypothesis, spectral responses of solar cells built with the same structure are needed.

6 ACKNOWLEDGEMENTS

The authors would like to thank T. Leimenstoll and F. Schätzle for process technology.

The experimental work was supported by the German Federal Ministry for the Environment, Nature Conservation, and Nuclear Safety under contract number 0329849A “Th-ETA”. The simulations as well as the e-beam processing were performed in the scope of the Nanovolt project (03SF0322F), supported by the German Federal Ministry of Education and Research as well as by the Deutsche Fortschungsgemeinschaft (PAK88).

7 REFERENCES

[1] M. A. Green, “Silicon solar cells Advanced Principles and Practice”, University of New South Wales, Sydney, 1995

[2] J. Zhao, M. A. Green, “Optimized antireflection Coatings for High-Efficiency silicon solar cells”, IEEE Trans. Electron Dev., Vol 38, No 8, 1991

[3] J. Zhao, A. Wand, P. P. Altermatt, S. R. Wenham, M. A. Green, “24% efficient PERL silicon solar cell: recent improvements in high efficiency silicon cell research”, Solar Energy Materials and solar Cells, 41/42, 87-99, 1996

[4] S. W. Glunz “High-efficiency crystalline silicon solar cells”, Adv. in OptoElectron. 97370/1-15 (2007)

[5] R. Morf, H. Kiess, C. Heine, Diffractive optics for solar cells, in: J. Turunen, F. Wyrowski (Eds.), Diffractive optics, akademie Verlag, Berlin, 1997

[6] H. Kiess, J. E. Epler, M. T. Gale, L. Krausbauer, R. Morf, W. Rehwald, “Light trapping with submicron gratings in thin crystalline silicon solar cells”, Proc. 10th Europ. PV Solar Energy Conf., Lisbon, 19-22, 1991

[7] H. Hauser et al. “Honeycomb textured multicrystalline silicon via NanoImprint Lithography”, Proc. of this conference, 2009